

Detection of Unusual Reaction Intermediates during the Conversion of $W(N_2)_2(dppe)_2$ to $W(H)_4(dppe)_2$ and of H_2O into H_2

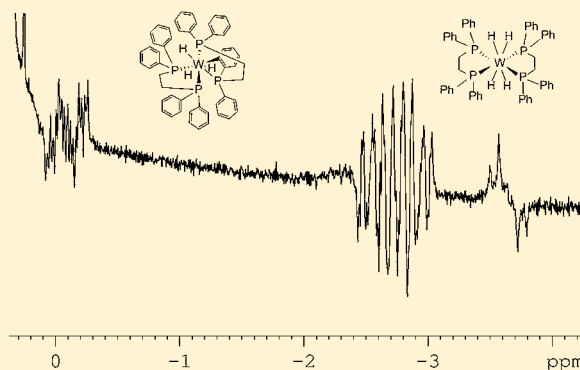
Beatriz Eguillor,[†] Patrick J. Caldwell,[†] Martin C. R. Cockett,[†] Simon B. Duckett,^{*,†} Richard O. John,[†] Jason M. Lynam,[†] Christopher J. Sleight,[†] and Ian Wilson[‡]

[†]Department of Chemistry, University of York, Heslington, York, U.K. YO10 5DD

[‡]Department of Safety of Medicines, AstraZeneca, Alderley Park, Macclesfield, Cheshire, U.K. SK10

Supporting Information

ABSTRACT: $W(N_2)_2(dppe-\kappa^2P)_2$ reacts with H_2 to form $WH_3\{Ph-(C_6H_4)PCH_2CH_2PPh_2-\kappa^2P\}(dppe-\kappa^2P)$ and then $W(H)_4(dppe-\kappa^2P)_2$. When *para*-hydrogen is used in this study, polarized hydride signals are seen for these two species. The reaction is complicated by the fact that trace amounts of water lead to the formation of H_2 , $PPh_2CH_2CH_2Ph_2P(O)$ and $W(H)_3(OH)(dppe-\kappa^2P)_2$, the latter of which reacts further via H_2O elimination to form $W(H)_4(dppe-\kappa^2P)_2$ and $[WH_3\{Ph(C_6H_4)PCH_2CH_2PPh_2-\kappa^2P\}(dppe-\kappa^2P)]$. These studies demonstrate a role for the 14-electron intermediate $W(dppe-\kappa^2P)_2$ in the CH activation reaction pathway leading to $[WH_3\{Ph(C_6H_4)PCH_2CH_2PPh_2-\kappa^2P\}(dppe-\kappa^2P)]$. UV irradiation of $W(H)_4(dppe-\kappa^2P)_2$ under H_2 led to phosphine dechelation and the formation of $W(H)_6(dppe-\kappa^2P)(dppe-\kappa^1P)$ rather than H_2 loss and $W(H)_2(dppe-\kappa^2P)_2$ as expected. Parallel DFT studies using the simplified model system $W(N_2)_2((Ph)HPCH_2CH_2PH_2-\kappa^2P)-(H_2PCH_2CH_2PH_2-\kappa^2P)$ confirm that *ortho*-metalation is viable via both $W(dppe-\kappa^2P)_2$ and $W(H)_2(dppe-\kappa^2P)_2$ with explicit THF solvation being necessary to produce the electronic singlet-based reaction pathway that matches with the observation of *para*-hydrogen induced polarization in the hydride signals of $[WH_3\{Ph(C_6H_4)PCH_2CH_2PPh_2-\kappa^2P\}(dppe-\kappa^2P)]$, $W(H)_3(OH)(dppe-\kappa^2P)_2$ and $W(H)_4(dppe-\kappa^2P)_2$ during this study. These studies therefore reveal the existence of differentiated and previously unsuspected thermal and photochemical reaction pathways in the chemistry of both $W(N_2)_2(dppe-\kappa^2P)_2$ and $W(H)_4(dppe-\kappa^2P)_2$ which have implications for their reported role in N_2 fixation.



INTRODUCTION

Systems such as $W(N_2)_2(dppe-\kappa^2P)_2$ (**1**) and $W(CO)_3(PCy_3)_2$ provide important examples of complexes where the activation of small molecules by inorganic compounds can be seen in action.¹ In the case of $W(N_2)_2(dppe-\kappa^2P)_2$, the binding of dinitrogen and the resulting sensitivity to electrophilic attack have particular relevance to nitrogen fixation.² $W(CO)_3(PCy_3)_2$, on the other hand, has provided a model system to enable the subsequent rationalization of dihydrogen activation in terms of both classical dihydride and dihydrogen interactions that are now ubiquitous to inorganic chemistry.^{3–6}

Reactivity studies involving $W(N_2)_2(dppe-\kappa^2P)_2$ ⁷ suggest the generation of coordinatively unsaturated $W(dppe-\kappa^2P)_2$ which has led to a range of novel reactions. These include the removal of CO from dimethylformide,⁸ and the conversion of benzaldehydeiminines into isocyanides.⁹ Studies have also demonstrated that the dppe ligand can be converted by this complex into the tetradentate phosphine *meso*-*o*- $C_6H_4(PPhCH_2CH_2PPh_2)_2$.¹⁰ Furthermore, unusual reactivity has also been observed in other tungsten phosphine systems.¹¹ Others have demonstrated that protonation of $W(N_2)_2(dppe-\kappa^2P)_2$ leads to a hydrazido complex, with ammonia subsequently formed under mild conditions.^{12,13} The involve-

ment of a second metal has also been shown to facilitate proton transfer.^{14,15}

The chemistry of tungsten polyhydride complexes containing mono and bidentate phosphine ligands has also been the subject of significant investigation,¹⁶ with many dihydride, tetrahydride and hexahydride complexes reported. However, as in the case of related polyhydride iridium systems,¹⁷ the mixing of η^2-H_2 and $M(H)_2$ coordination modes adds significantly to the complexity of ligand binding. This results in an array of $W(0)$ – $W(VI)$ complexes and difficulties in their unambiguous characterization. Utilization of $T_{1(\min)}$ values as a route to achieve this differentiation is well established.^{18,19} For example, NMR data for $WH_6(PPh(CH_2CH_2PPh_2))_2$ has produced T_1 values of 103 and 126 ms at 223 K which suggests classical hexahydride formulation.²⁰ The protonated form of this complex, $[W(H)_{7-2x}(\eta^2-H_2)_x(PPh(CH_2CH_2PPh_2))_2]BF_4$ ($x = 1$ or 2) was, however, found to yield a T_1 value of 21 ms at 223 K which is consistent with the involvement of exchanging η^2-H_2 ligands. Related protonation studies on the classical tetrahydride $W(H)_4(PMePh_2)_4$ lead to initial attack on the hydrido

Received: March 6, 2012

Published: October 16, 2012

ligand to generate $[\text{WH}_3(\eta^2\text{-H}_2)(\text{PMePh}_2)_4]^+$ which subsequently rearranges to give the pentahydride.^{21,15}

Factors that control the binding of small molecules to $\text{W}(\text{CO})_3(\text{PCy}_3)_2$ and its agostic bonding within the cyclohexyl moiety have been explored by density functional theory (DFT).²² The use of DFT to probe aromatic C–H bond activation at tungsten²³ and to examine polyhydride systems has also been shown to enable rationalization of the reactivity of such systems.²⁴ Others have modeled the complex functionalization of N_2 by H_2 in such organometallic systems.²⁵ Furthermore, the interaction of hydride ligands with water has been shown to result in the generation of a metal–hydroxide complex and dihydrogen.²⁶ Such DFT methods are particularly useful in predicting the reactivity of reaction intermediates that are normally experimentally undetectable.

NMR spectroscopy, in conjunction with UV photolysis of samples within the NMR probe, has enabled the characterization of very unstable materials and the monitoring of their reactivity. This approach has been used successfully to detect unstable alkyl hydride^{27,28} complexes, a xenon complex²⁹ and a number of hydride complexes.³⁰ More recently, the approach has been used to generate unstable tungsten dihydrogen complexes.³¹ The related technique of photo-Chemically Induced Dynamic Nuclear Polarization (photo-CIDNP) has been used to determine kinetic parameters for protein folding.³²

The *in situ* photochemical method has been extended to enable the successful detection of materials that are unstable even at 213 K through the signal enhancement resulting from the *para*-hydrogen (*para*- H_2)^{33,34} induced polarization effect (PHIP),^{33–35} an approach which has been reviewed recently.³⁶ In the present paper, we report first on a study of $\text{W}(\text{H})_2(\text{CO})_3(\text{PCy}_3)_2$ using the *in situ* photolysis method whose objective was to establish whether equilibration between a metal $\eta^2\text{-H}_2$ complex and its dihydride counterpart could be followed using PHIP. The reactivity of the complex $\text{W}(\text{N}_2)_2(\text{dppe-}\kappa^2\text{P})_2$ (**1**) toward H_2 is then followed using PHIP and a number of interesting observations are described. The resulting complexes are characterized by full NMR analysis including ^{183}W NMR data.^{37,38} These studies are rationalized through model DFT calculations based on $\text{W}(\text{N}_2)_2((\text{Ph})\text{-HPCH}_2\text{CH}_2\text{PH}_2\text{-}\kappa^2\text{P})(\text{H}_2\text{PCH}_2\text{CH}_2\text{PH}_2\text{-}\kappa^2\text{P})$ (**1m**) where the dppe ligand is replaced by a simplified phosphine.

EXPERIMENTAL SECTION

General Conditions and Materials. All manipulations were carried out under inert atmosphere conditions, using standard Schlenk techniques (with N_2 or Ar as the inert atmosphere) or high vacuum techniques. Solvents were obtained as analytical grade from Fisher. The WCl_6 used was obtained from Acros Organics and the *bis*-(1,2-diphenyl-phosphino)ethane (dppe) was obtained from Sigma-Aldrich and used without further purification. $\text{W}(\text{N}_2)_2(\text{dppe-}\kappa^2\text{P})_2$ (**1**) was prepared by known literature methods⁷ and characterized by NMR. NMR spectra were collected on Bruker DRX 400, Avance 600 and Avance II 700 spectrometers.

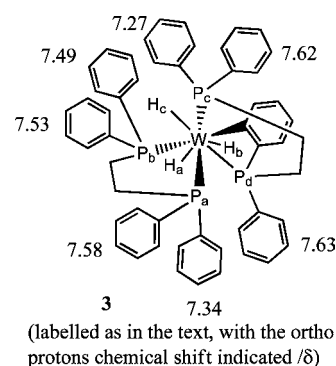
Preparation and Characterization of $\text{W}(\text{H})_4(\text{dppe-}\kappa^2\text{P})_2$ (2**).** An NMR sample of **1** was prepared by charging a 5 mm NMR tube fitted with a Young's tap with ca. 1 mg of **1** and then adding toluene- d_8 via vacuum transfer. Hydrogen (3 atm) was then added to this sample at room temperature. After 2 h of heating at 328 K, the $^{31}\text{P}\{^1\text{H}\}$ NMR spectrum of the resultant solutions showed only a singlet at 61.0 ppm due to the known complex **2**. The room temperature NMR data for **2** agree with that in the literature.³⁹ We note an increase in the T_1 value to 585 ms when recorded with ^{31}P decoupling at 258 K, in accordance with a classical tetrahydride configuration for **2**.

^1H NMR (700 MHz, THF- d_8 , 283 K): δ 7.90 (bs, $J_{\text{HH}} = 7.3$ Hz, 8H, Ph-*ortho*), 7.21 (t, $J_{\text{HH}} = 7.3$ Hz, 8H, Ph-*meta*), 7.17 (m, $J_{\text{HH}} = 7.0$ Hz, 8H, Ph-*ortho*), 7.15 (m, $J_{\text{HH}} = 7.3$ Hz, 4H, Ph-*para*), 6.76 (m, $J_{\text{HH}} = 7.0$ Hz, 8H, Ph-*meta*), 6.79 (t, $J_{\text{HH}} = 7.0$ Hz, 4H, Ph-*para*), 2.68 (dd, $J_{\text{HP}} = 28.6$ Hz, $J_{\text{HH}} = 9$ Hz, 4H, $-\text{CH}_2-$), 1.70 (m, $J_{\text{HH}} = 9$ Hz, 4H, $-\text{CH}_2-$), -3.68 (binomial quintet, $J_{\text{HP}} = 26$ Hz, $J_{\text{WH}} = 38$ Hz, 4H). $^{13}\text{C}\{^1\text{H}\}$ NMR (176.008 MHz, THF- d_8 , 283 K): δ 143.81 (d, $J_{\text{CP}} = 39.7$ Hz C_{ipso}), 139.26 (d, $J_{\text{CP}} = 32.5$ Hz C_{ipso}), 137.19 (Ph-*ortho*), 134.44 (Ph-*ortho*), 128.8 (Ph-*para*), 127.35 (Ph-*meta*), 127.14 (Ph-*para*), 127.03 (Ph-*meta*) 34.76 (d, $J_{\text{CP}} = 32.5$ Hz $-\text{CH}_2-$). $^{31}\text{P}\{^1\text{H}\}$ NMR (283.4 MHz, THF- d_8 , 283 K): 61.5 s ($J_{\text{WP}} = 169$ Hz). T_1 (min) (WH, 400 MHz, C_7D_8): 79 ± 1.1 ms (signal at $\delta -3.63$, temperature 273 K). $^{183}\text{W}\{^1\text{H}\}$ NMR (16.6 MHz, C_7D_8 , 298 K): $\delta -3354.5$ (m, $J_{\text{WP}} = 167.3$ Hz).

NMR Scale Preparation of $[\text{W}(\text{H})_3(\text{Ph}(\text{C}_6\text{H}_4)\text{PCH}_2\text{CH}_2\text{PPh}_2\text{-}\kappa^2\text{P})_2(\text{dppe-}\kappa^2\text{P})]$ (3**).** A sample of **1** was dissolved in toluene- d_8 and placed in a dry ice/isopropanol bath at ca. 230 K. The tube was then pressurized to 3 atm with hydrogen and the resulting sample irradiated at 223 K using a broadband 180 W Oriel UV lamp for 40 min. At this point NMR spectroscopy revealed that the sample contained **3** (see below) at >90% conversion. This process enabled the characterization of **3** to be completed at low temperature by COSY, NOE and HMQC methods where its lifetime was sufficiently extended. Full NMR data for **3** are presented in Tables 1 and s1. $^{183}\text{W}\{^1\text{H}\}$ NMR (16.6 MHz, C_7D_8 , 298 K): $\delta -2917$.

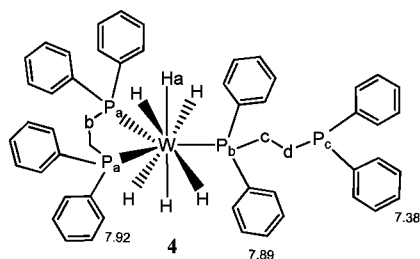
Table 1. Partial NMR Data for **3 in Toluene- d_8 , 298 K**

group, chemical shift δ , J (/Hz) (T_1)	coupling to P_a (J/Hz)	coupling to P_b (J/Hz)	coupling to P_c (J/Hz)	coupling to P_d (J/Hz)
H_{ar} , -0.14 , $J_{\text{HaHc}} = 2$, $J_{\text{HaHb}} = 4$ (T_1 773 ms at 248 K)	24	68	34	8
H_{br} , -2.69 , $J_{\text{HbHc}} = 8$ (T_1 724 ms at 248 K)	62	26	12	22
H_{cr} , -2.93 , J_{HH} as above (T_1 510 ms at 248 K)	6	24	64	38
P_b , 59.3, $J_{\text{WP}} = 138$	8	--	15	8
P_c , 47.4, $J_{\text{WP}} = 170$	76	15	--	8
P_{ar} , 55.4, $J_{\text{WP}} = 180$	-	8	76	22
P_{br} , -13.2 , $J_{\text{WP}} = 122$	22	8	8	-



NMR Scale Preparation of $[\text{W}(\text{H})_6(\text{dppe-}\kappa^2\text{P})(\text{dppe-}\kappa^1\text{P})]$ (4**).** A sample of **2** in toluene- d_8 was cooled to 260 K, and then pressurized to 3 atm by hydrogen gas. The cooled sample was then exposed to UV irradiation (Oriel lamp) for 120 min. At this point, NMR spectroscopy revealed the sample to contain both **4** (see below) and **2** with no evidence for **3** even though it had already been demonstrated to be sufficiently thermally and photochemically stable under these conditions. The ratio of **4** to **2** was found to be 1:1 at this point and remained unchanged at this level after 30 min of further irradiation. This route enabled the subsequent characterization of **4** at 273 K by COSY, NOE and HMQC methods. ^1H NMR (700 MHz, toluene- d_8 , 273 K): δ 2.24 (m, $J_{\text{PH}} = 18$ Hz, H_b), δ 7.92 (ortho), δ 7.04

(meta), δ 7.00 (para), δ 2.67 (H_c) δ 7.82 (ortho), δ 6.98 (meta), δ 7.00 (para), δ 2.79 (m, H_d) δ 7.38 (ortho), δ 7.00 (meta), δ 7.03 (para); δ -2.41 (dq, $J_{\text{WH}} = 38.1$ Hz, $J_{\text{HP(a)}} = 36.3$ Hz, $J_{\text{HP(b)}} = 26.5$ Hz, H_{a} , $^{13}\text{C}\{^1\text{H}\}$ NMR (176.008 MHz, toluene-*d*₈, 273K), attached to P_a, δ 31.85 (d) $J_{\text{CP}} = 47$ Hz, δ 139.52 (ipso), δ 133.12 (ortho), δ 128.04 (meta), δ 129.04 (para), attached to P_b, δ 34.60 (d) $J_{\text{CP}} = 18$ Hz, δ 139.41 (ipso), δ 132.96 (ortho), δ 127.23 (meta), δ 128.27 (para), attached to P_c, δ 34.80 (d) $J_{\text{CP}} = 33$ Hz, δ 132.93 (ortho), δ 129.09 (meta), δ 128.02 (para). $^{31}\text{P}\{^1\text{H}\}$ NMR (283.4 MHz, toluene-*d*₈, 273K), P_a, δ 54.7, $J_{\text{WH}} = 95$ Hz, $J_{\text{P(a)P(b)}} = 7.4$ Hz, P_b, δ 42.3, $J_{\text{WH}} = 62$ Hz, $J_{\text{P(a)P(b)}} = 7.4$ Hz, $J_{\text{P(b)P(c)}} = 38$ Hz, P_c, δ -12.4, $J_{\text{P(b)P(c)}} = 38$ Hz; (16.6 MHz, C₇D₈, 298 K), T₁(min) (WH, C₇D₈): 890 ms (signal at δ -2.41, temperature 228 K). $^{183}\text{W}\{^1\text{H}\}$ NMR (16.6 MHz, C₇D₈, 298 K), δ -4000 (m).



(labelled as in the text, ortho proton chemical shift indicated / δ)

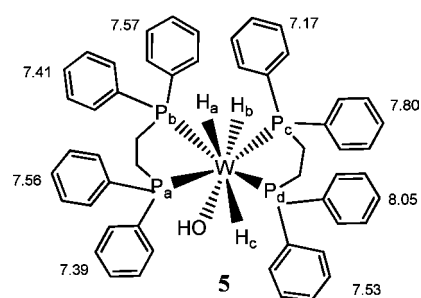
NMR Scale Preparation of $\text{W}(\text{H})_3(\text{OH})(\text{dppe-}\kappa^2\text{P})_2$ (5). A sample of **1** was dissolved in undried toluene-*d*₈ and left to stand overnight at room temperature. Three atm. of hydrogen was then added and left to react for a further 24 h. During this period, NMR signals due to **5** (see below) became evident. The ratio of **5** to **1** typically reached 1:5 after 24 h. Over a longer time period, the slow thermal conversion of **5** into both **4** and **2** (ratio ca. 1:20) occurred. Signals for compound **3** were also observed, in addition to those of free $\text{PPh}_2\text{CH}_2\text{CH}_2\text{PPh}_2(\text{O})$. This method allowed the production of sufficient **5** for its full NMR characterization at 283 K by COSY, NOE and HMQC methods. A sample where **5** is the dominant product can be obtained from a similar reaction in THF when it is doped with H₂O. Full NMR data for **5** are presented in Tables 2 and s2

Table 2. Partial NMR Data for 5

group, chemical, shift/ δ (multiplicity) and T ₁ at 268 K	coupling to P _a (J/Hz)	coupling to P _b (J/Hz)	coupling to P _c (J/Hz)	coupling to P _d (J/Hz)
H _a , -2.26 (t); 284 ms	18	38	62	30
H _b , -2.37 (dd); 282 ms	62	44	18	24
H _c , 1.59 (ddd)	30	114	30	86
OH, -3.00 (bs); 744 ms				
P _b , 64.0 (bs)	16	-	16	21.6
P _c , 45.7 (AB spin system $J_{\text{AB}} 152$, $\Delta\nu 496.5$ Hz)	152	14	-	14
P _a , 47.6 (AB spin system)	-	14	152	14
P _d , 36.9 (bt)	9	21.6	9	-

RESULTS AND DISCUSSION

Photochemical Reactions of $\text{W}(\text{CO})_3(\text{PCy}_3)_2$ with *para*-Hydrogen. A sample of $\text{W}(\text{CO})_3(\text{PCy}_3)_2$ was prepared and then reacted with *para*-H₂, with the ensuing thermal reaction monitored by ^1H NMR spectroscopy. While hydride signals for the dihydride isomer, $\text{W}(\text{H})_2(\text{CO})_3(\text{PCy}_3)_2$, were observed at 298 K, they failed to exhibit any PHIP. We then employed the *in situ* UV photolysis method to monitor this reaction directly at 213 K using 325 nm radiation. However, while the hydride signals for $\text{W}(\text{H})_2(\text{CO})_3(\text{PCy}_3)_2$ were detected, no PHIP was seen in the two hydride resonances. We conclude therefore that



(labelled as in the text, with ortho proton chemical shift indicated / δ)

the rapid relaxation associated with the $\eta^2\text{-H}_2$ isomer quenches the PHIP effect in this system during tautomerization between the $\text{W}(\text{H})_2(\text{CO})_3(\text{PCy}_3)_2$ and $\text{W}(\text{H})_2(\text{CO})_3(\text{PCy}_3)_2$ forms. This result contrasts with that previously reported Bargon et al. who showed that an organic hydrogenation product can show PHIP even though it is formed via a metal-based intermediate that exists in an $\eta^2\text{-H}_2$ form.⁴⁰ In both cases, the lifetime of the $M\text{-}\eta^2\text{-H}_2$ intermediate must play a pivotal role in determining the extent of polarization in any newly formed hydrogenation product. Consequently, we decided to extend the study to target $\text{W}(\text{H})_4(\text{dppe-}\kappa^2\text{P})_2$ (**2**).

Reactions of $\text{W}(\text{N}_2)_2(\text{dppe-}\kappa^2\text{P})_2$ (1**) with *para*-Hydrogen.** $\text{W}(\text{N}_2)_2(\text{dppe-}\kappa^2\text{P})_2$ (**1**) reacts with H₂ to form $\text{W}(\text{H})_4(\text{dppe-}\kappa^2\text{P})_2$ (**2**),⁴¹ and when this reaction was followed in THF-*d*₈ with *para*-H₂ at 333 K, the resulting ^1H NMR spectrum contains a polarized hydride signal at δ -3.66 as shown in Figure 1a. This hydride signal appears as a quintet

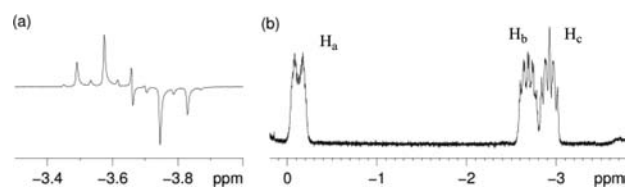


Figure 1. Selected ^1H NMR signals observed during reactions of $\text{W}(\text{N}_2)_2(\text{dppe-}\kappa^2\text{P})_2$ (**1**) and H₂. (a) PHIP polarized hydride signal for $\text{W}(\text{H})_4(\text{dppe-}\kappa^2\text{P})_2$ (**2**), (b) hydride signals, H_a, H_b and H_c of $[\text{WH}_3\{\text{Ph}(\text{C}_6\text{H}_4)\text{PCH}_2\text{CH}_2\text{PPh}_2\text{-}\kappa^2\text{P}\}(\text{dppe-}\kappa^2\text{P})]$ (**3**).

with $J_{\text{PH}} = 28$ Hz and is flanked by ^{183}W satellites with $J_{\text{HW}} = 38$ Hz. A 2D $^1\text{H}\text{-}^{183}\text{W}$ HMQC³⁷ spectrum was then recorded and showed a ^{31}P coupled multiplet at δ -3363 when referenced to TMS at 100 MHz.⁴²

The origin of the PHIP enhancement seen in the NMR signal observed for the hydride ligands of **2** results from the second order $[\text{AX}]_4$ spin system which provides the magnetic inequivalence necessary to achieve PHIP activity.⁴³ Interestingly, weak PHIP polarization is also seen in one of the two sets of *ortho*-phenyl proton resonances of **2** that appears at δ 7.42 where $J_{\text{PH}} = 8$ Hz; the antiphase coupling reflected in the PHIP enhancement is -3 Hz. This observation provides insight into the intramolecular activation of the dppe-ligand (*q.v.*). The corresponding ^1H COSY NMR spectrum of **2** contained a weak connection between the hydride resonance and the dppe backbone ^1H signals at δ 2.64 in addition to the *ortho*-phenyl proton signal at δ 7.42 thereby confirming that they are all weakly scalar coupled.

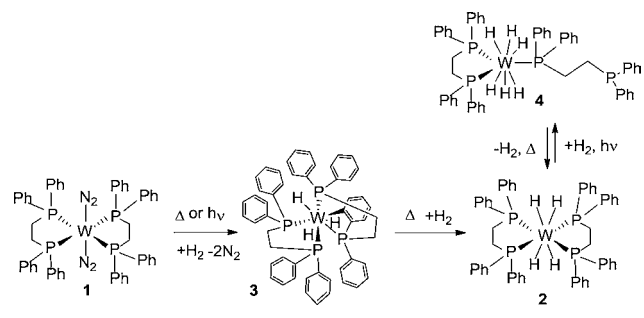
Previous studies have shown that PHIP can be used to examine successfully a range of mono-, di- and trihydride

complexes.⁴⁴ The hydride ligand polarization observed in **2** and reported here represents the first time that PHIP has been seen in such a mononuclear tetrahydride complex. The $T_{1(\text{min})}$ value of the hydride signal of **2** was determined as 0.58 s at 258 K and is fully consistent with the observation of PHIP in this species. We conclude therefore that any $W-\eta^2\text{-H}_2$ based reaction intermediate which might exist on the reaction pathway to **2** has a very short lifetime (see DFT discussion later).^{20,45}

We expected this reaction to proceed via the intermediate $W(\text{H})_2(\text{N}_2)(\text{dppe-}\kappa^2\text{P})_2$ but this was not detected at 333 K. We therefore re-examined the reaction at the lower temperature of 295 K where we observed two further sets of polarized hydride signals in the corresponding ^1H NMR spectrum at δ -2.69 and δ -2.93 (see Figure 1b). These resonances are due to the new complex, **3**, and proved to couple to a third hydride resonance at δ -0.14 according to COSY methods. These data therefore preclude the detection of $W(\text{H})_2(\text{N}_2)(\text{dppe-}\kappa^2\text{P})_2$ and suggest that an unexpected reaction has taken place.

Photochemical Reactions of $W(\text{N}_2)_2(\text{dppe-}\kappa^2\text{P})_2$ (1**) with *para*-Hydrogen.** We describe now how the identity of **3**, an intramolecular CH bond activation product, was confirmed through its formation in a series of low temperature irradiation studies. The formation of **2** and **3** from **1** is illustrated in Scheme 1. The 297 nm irradiation of **W-**

Scheme 1. Reaction Products and Pathways Involved in the Reactions of $W(\text{N}_2)_2(\text{dppe-}\kappa^2\text{P})_2$ (1**) with H_2**



$(\text{N}_2)_2(\text{dppe-}\kappa^2\text{P})_2$ has previously been suggested to produce $W(\text{dppe-}\kappa^2\text{P})_2$ as the sole photoproduct.⁴¹ It subsequently forms $W(\text{N}_2)(\text{dppe-}\kappa^2\text{P})_2$ and then $W(\text{N}_2)_2(\text{dppe-}\kappa^2\text{P})_2$ upon back-reaction with N_2 , although ^{15}N labeling suggests a similar sequential pathway for the original ligand loss process.⁴⁶ The first of the studies reported here was completed using *in situ* irradiation of a sample of **1** under an atmosphere of H_2 within the NMR system at 233 K using a 325 nm HeCd laser.

One dominant photoproduct, **3** was evident in the resulting NMR spectra, and with *para*- H_2 , the associated ^1H NMR spectra contain the same three hydride resonances all of which exhibited a strong PHIP effect. On the basis of the intensities of the PHIP enhanced signals, we conclude that H_2 addition to the sites giving rise to the δ -2.69 and δ -2.93 signals is dominant. Under these conditions, a weakly polarized hydride signal for **2** was also seen (Figure 2).

Characterization of $W\text{H}_3\{\text{Ph}(\text{C}_6\text{H}_4)\text{PCH}_2\text{CH}_2\text{PPh}_2\text{-}\kappa^2\text{P}\}(\text{dppe-}\kappa^2\text{P})$ (3**).** External UV irradiation of a similar sample at 223 K using a 180 W Oriel UV lamp was then used to produce an NMR sample that was found to contain essentially **3** (Figure 1b illustrates the hydride region of the resulting ^1H NMR spectrum). This enabled the complete low temperature NMR characterization of **3** via COSY, NOE and HMQC methods. Notably, the three hydride signals of **3** now clearly

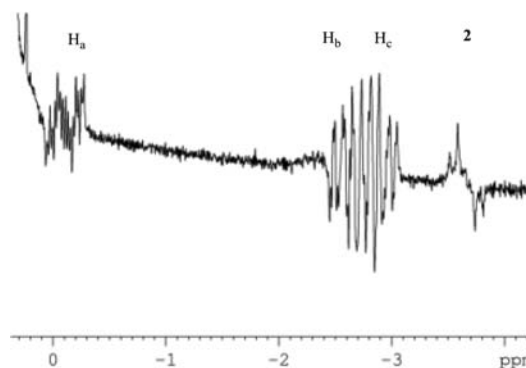


Figure 2. PHIP enhanced NMR signals observed during the generation of $W(\text{H})_4(\text{dppe-}\kappa^2\text{P})_2$ (**2**) and $[W\text{H}_3\{\text{Ph}(\text{C}_6\text{H}_4)\text{PCH}_2\text{CH}_2\text{PPh}_2\text{-}\kappa^2\text{P}\}(\text{dppe-}\kappa^2\text{P})]$ (**3**) under *in situ* photolysis at 298 K.

possess 1:1:1 integrals with 8 further distinct ethane bridge protons also evident. Examination of a series of NMR spectra revealed 39 aromatic proton resonances for **3** which arise from seven sets of five coupled signals due to a phenyl ring and one set of four coupled signals due to a CH bond activated phenyl ring. In addition to this, **3** yields four ^{31}P NMR signals that are located at δ -13.2 , 47.4, 55.4 and 59.3.

The ^{31}P NMR signal for free dppe appears at δ -12.8 , close to one of the resonances of **3** at δ -13.2 . This suggests that **3** may contain a phosphorus center that is no longer coordinated to the metal. However, the resonance at δ -13.2 couples strongly (64 Hz) to the hydride ligand that resonates at δ -2.63 in the ^1H NMR spectrum of **3**. It is therefore clear that the phosphorus center giving rise to this signal is bound to the metal. Such a high-field signal for a metal-bound phosphorus atom has precedence as similar shifts are observed for metallo-phosphorus 4-membered rings.⁴⁷ A ^{13}C resonance at δ 122.33 in **3** corresponds to a quaternary carbon directly attached to the tungsten center and supports this *ortho*-metalation concept.

We conclude therefore that **3** is the trihydride complex $W\text{H}_3\{\text{Ph}(\text{C}_6\text{H}_4)\text{PCH}_2\text{CH}_2\text{PPh}_2\text{-}\kappa^2\text{P}\}(\text{dppe-}\kappa^2\text{P})$ where one of the phosphine ligands is *ortho*-metalated. This species is shown in Scheme 1 and exhibits $T_{1(\text{min})}$ values for its three hydride resonances of 0.77, 0.77, and 0.51 s, respectively, at 248 K. These values serve to confirm that **3** is a classical W(IV) trihydride which explains why PHIP enhancement can be observed in its hydride signals.²⁰ The ^{183}W signal of **3** appears as a ^{31}P -coupled multiplet at δ -2913 which proves to be close to that of **2** thereby supporting their similar oxidation state and 18 electron counts.

Conversion of $W\text{H}_3\{\text{Ph}(\text{C}_6\text{H}_4)\text{PCH}_2\text{CH}_2\text{PPh}_2\text{-}\kappa^2\text{P}\}(\text{dppe-}\kappa^2\text{P})$ (3**) to $W(\text{H})_4(\text{dppe-}\kappa^2\text{P})_2$ (**2**).** The slow conversion of **3** into the tetrahydride complex **2** was found to occur upon warming a solution of **3** in toluene- d_8 in the presence of 3 atm H_2 . However, a new hydride resonance due to a further species, **4**, was also detected at δ -2.4 (Figure 3a) in these experiments, although at a level of less than 5% conversion. The conversion of **3** to **2** requires the reformation of the activated CH bond which in turn offers an explanation for the observation of PHIP in the *ortho*-phenyl proton resonance of **2** at δ 7.42 as described earlier; a *para*- H_2 derived proton is placed in this site through this exchange process.

Kinetic Studies on the Conversion of **3 to **2**.** When this conversion was monitored in THF- d_8 under 3 atm of H_2 , only **2** is formed with a rate constant for conversion at 293 K of $4.2 \times 10^{-5} \text{ s}^{-1}$. This reaction was then monitored over the

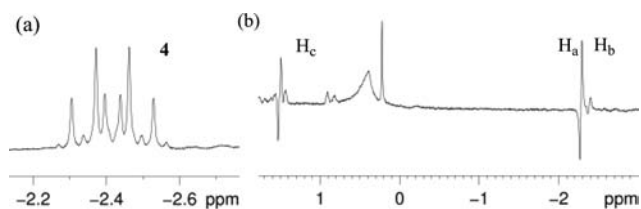


Figure 3. (a) ^1H hydride ligand NMR signal for $\text{W}(\text{H})_6(\text{dppe-}\kappa^2\text{P})$ (**4**) and (b) three ^{31}P decoupled PHP polarized hydride signals seen for $\text{W}(\text{H})_3(\text{OH})(\text{dppe-}\kappa^2\text{P})$ (**5**).

temperature range 283–323 K and ΔH^\ddagger and ΔS^\ddagger values of $79 \pm 3 \text{ kJ mol}^{-1}$ and $-54 \pm 11 \text{ J K}^{-1} \text{ mol}^{-1}$, respectively, were determined from the associated rate data. These values are consistent with a transition state that involves a reduction in the number of species present and hence a contribution from H_2 binding in the rate limiting step. Furthermore, when this reaction is completed with D_2 rather than H_2 at 293 K, while there is no evidence for D incorporation into **3**, $k_{\text{H}}/k_{\text{D}}$ is 1.09 which supports the involvement of H_2 in this pathway. The corresponding values of ΔH^\ddagger and ΔS^\ddagger for the reaction of **3** with D_2 are $70.6 \pm 10 \text{ kJ mol}^{-1}$ and $-85 \pm 32 \text{ J K}^{-1} \text{ mol}^{-1}$, respectively. The value of ΔG^\ddagger (300) for the reaction with D_2 was determined as 96.2 kJ mol^{-1} compared with that of 95.0 kJ mol^{-1} for reaction with H_2 which confirms that an interaction with the incoming ligand helps lower the barrier to this reaction. The rate data that are used to determine these values is presented in Table 3. The associated Eyring plot, and a

Table 3. Rate Data for the Conversion of **3** into **2** through Reaction with H_2 and D_2 , Respectively

temperature/K	k_{H}/s	k_{D}/s
283	9.75×10^{-6}	9.29×10^{-6}
293	4.19×10^{-5}	3.84×10^{-5}
303	1.27×10^{-4}	5.08×10^{-5}
313	2.98×10^{-4}	2.40×10^{-4}
323	9.73×10^{-4}	4.39×10^{-4}

typical kinetic trace are presented in Figure 4. The kinetic data that are presented in Figure 4 was recorded at 293 K and corresponds to monitoring the conversion of complex **3** into **2**.

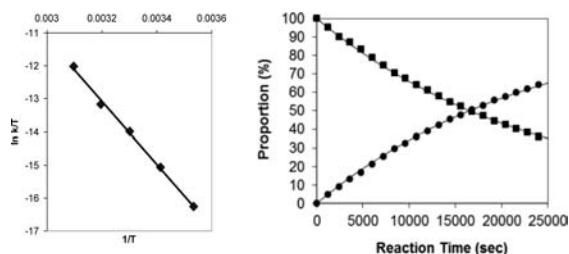


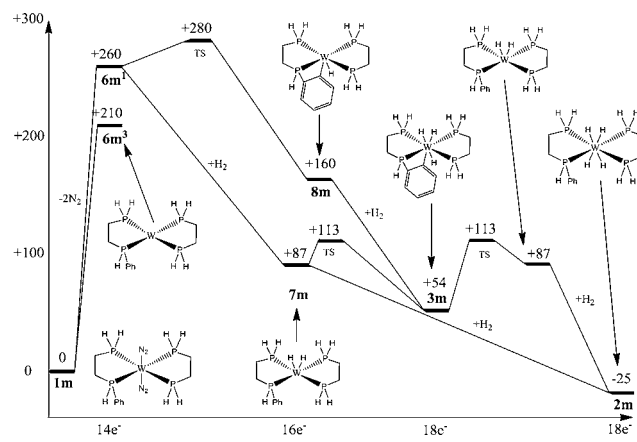
Figure 4. (a) Eyring plot for the conversion of **3** into **2**; (b) kinetic trace showing how the proportions of **3** (■) and **2** (●) change with reaction time (sec) at 293 K.

It should be noted that in the absence of H_2 , **3** decomposes, while also forming a new hydride-containing species. This complex is highly fluxional but decomposes on exposure to H_2 rather than forming **2** or **3**. At 263 K, two mutually coupled hydride resonances are visible at $\delta -0.82$ and -1.03 . The corresponding ^{183}W signal of this species appears at $\delta -2245$. Despite our best efforts, we have not been able to identify it

conclusively, and while a $\text{W}(\text{H})_2(\text{dppe-}\kappa^2\text{P})_2$ formulation would match with the spectroscopic data, the DFT study now described suggests that this is not the case.

Mapping of the Reaction Pathway of $\text{W}(\text{N}_2)_2(\text{dppe-}\kappa^2\text{P})_2$ (1**) with Hydrogen.** To rationalize these reactions further, a series of DFT calculations was performed on the model system $\text{W}(\text{N}_2)_2((\text{Ph})\text{HPCH}_2\text{CH}_2\text{PH}_2-\kappa^2\text{P})-(\text{H}_2\text{PCH}_2\text{CH}_2\text{PH}_2-\kappa^2\text{P})$ (**1m**) for which the dppe ligands has been replaced by the simplified phosphine ligands indicated. An optimized DFT structure for **1m** was computed using implicit solvation for THF. The structural features of **1m** correspond well with those of **1** as detailed in the Supporting Information. This structure was used as a starting point in a subsequent geometry optimization calculation of the *bis*- N_2 loss-product $\text{W}((\text{Ph})\text{HPCH}_2\text{CH}_2\text{PH}_2-\kappa^2\text{P})(\text{H}_2\text{PCH}_2\text{CH}_2\text{PH}_2-\kappa^2\text{P})$ (**6m**). The most stable geometry exists as a triplet ground state **6m³**, which lies 210 kJ mol^{-1} above **1m** in Gibbs Free Energy terms (Scheme 2, further reactivity, however, is via **6m¹**, the

Scheme 2. DFT Reaction Coordinate Profile for the Conversion of **1m** into **2m** without Specific THF Involvement

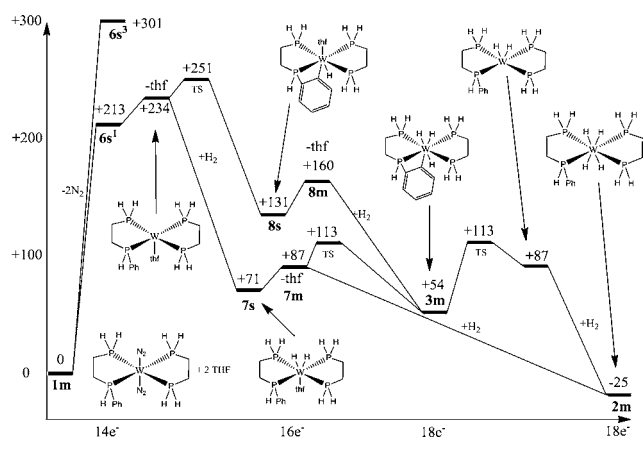


singlet). Oxidative addition of H_2 then proceeds to form the classical dihydride complex $\text{W}(\text{H})_4((\text{Ph})\text{HPCH}_2\text{CH}_2\text{PH}_2-\kappa^2\text{P})(\text{H}_2\text{PCH}_2\text{CH}_2\text{PH}_2-\kappa^2\text{P})$ (**2m**) which lies 25 kJ mol^{-1} below **1m** in a barrierless reaction involving the end-on approach of H_2 . Similar behavior has been reported in other systems.⁴⁸

The addition of a second molecule of H_2 to **7m** then forms the expected tetrahydride product $\text{W}(\text{H})_4((\text{Ph})\text{HPCH}_2\text{CH}_2\text{PH}_2-\kappa^2\text{P})(\text{H}_2\text{PCH}_2\text{CH}_2\text{PH}_2-\kappa^2\text{P})$ (**2m**) which lies 25 kJ mol^{-1} below **1m** in a barrierless reaction. Significantly, the formation of $\text{W}(\text{H})_3\{(\text{C}_6\text{H}_4)\text{HPCH}_2\text{CH}_2\text{PH}_2-\kappa^2\text{P}\}-(\text{H}_2\text{PCH}_2\text{CH}_2\text{P}(\text{H})_2-\kappa^2\text{P})$ (**3m**) occurs via *ortho*-metalation of **7m** via a 26 kJ mol^{-1} transition state. **3m** is, however, 33 kJ mol^{-1} lower in energy than **7m** and therefore corresponds to a thermodynamically viable product in accordance with the experimental observation of **3**. **3m** can also be formed in a reaction sequence that first involves CH activation (to form **8m**) from **6m¹**, where the barrier to *ortho*-metalation is now 20 kJ mol^{-1} , and then H_2 addition.

However, the explicit solvation of **6m³** with THF yields the complex $\text{W}((\text{Ph})\text{HPCH}_2\text{CH}_2\text{PH}_2-\kappa^2\text{P})(\text{H}_2\text{PCH}_2\text{CH}_2\text{PH}_2-\kappa^2\text{P})(\text{THF})_2$ which exists in its most stable form as a singlet (**6s¹**), 88 kJ mol^{-1} more stable than the triplet, **6s³**, and just 3 kJ mol^{-1} less stable than **6m³** (Scheme 3). Given that the experimental reaction is carried out in THF, it is reasonable to assume that **6s¹** exists in solution. Following loss of a single THF ligand from **6s¹**, oxidative addition of H_2 proceeds to form

Scheme 3. DFT Reaction Coordinate Profile for the Conversion of **1m into **2m** with Specific THF Involvement**



the classical dihydride complex **7s** in a barrierless reaction involving the end-on approach of H_2 . In this scenario, THF clearly plays an important role in stabilizing the dihydride complex $W(H)_2((Ph)HPCH_2CH_2PH_2-\kappa^2P)(H_2PCH_2CH_2PH_2-\kappa^2P)(THF)$ (**7s**) over its unsolvated 16-electron counterpart **7m**.

These DFT results are consistent with the experimental observation of PHIP in the hydride resonances of both **2** and **3** when explicit THF solvation is included, and confirm that there is little contribution from any $W-\eta^2-H_2$ type species on the reaction coordinate which connects **1** with **2**. We note that, in support of this deduction, $Ru(dppe-\kappa^2P)(CO)_2$ does indeed add H_2 via the electronic singlet intermediate, with PHIP being detected in the resulting hydride NMR signals.⁴⁹ In contrast, the analogous intermediate $Fe(dppe-\kappa^2P)(CO)_2$ has been shown by DFT to exist as a triplet which is consistent with the failure to observe PHIP for $Fe(H)_2(dppe-\kappa^2P)(CO)_2$.⁴⁹

An alternative mechanism involving loss of a single N_2 from **1m**, yields the 16-electron complex $W(N_2)((Ph)HPCH_2CH_2PH_2-\kappa^2P)(H_2PCH_2CH_2PH_2-\kappa^2P)$ for which a similar barrier exists to *ortho*-metalation as that determined for the equivalent THF complex, $W((Ph)HPCH_2CH_2PH_2-\kappa^2P)(H_2PCH_2CH_2PH_2-\kappa^2P)(THF)$. However, formation of the N_2 *ortho*-metalation product is thermodynamically unfavorable with respect to $W(N_2)((Ph)HPCH_2CH_2PH_2-\kappa^2P)(H_2PCH_2CH_2PH_2-\kappa^2P)(THF)$. Computed binding enthalpies for the first and second N_2 ligands of **1m** are 214 and 129 $kJ\ mol^{-1}$, respectively. This is consistent with the experimental observation that the rate of binding of the second N_2 ligand occurs much slower than that of the first.⁵⁰ Furthermore, when coupled with the relative thermodynamic instability of the N_2 *ortho*-metalation product, an explanation emerges for why no net photochemistry is observed for **1** in the absence of H_2 .

Formation of $W(H)_6(dppe-\kappa^2P)(dppe-\kappa^1P)$ (4**) by UV Irradiation of $W(H)_4(dppe-\kappa^2P)_2$ (**2**).** The chemistry discussed so far is further complicated by the fact that UV irradiation of a preformed sample containing **3** under H_2 at 295 K leads to the detection of both **2** and **4**. In contrast, irradiation of **1** with H_2 at 295 K results in the dominant photoproduct **2** with much lower levels of **3** and **4**. All four of these species are therefore photochemically active under these conditions.

When **2** is irradiated under an H_2 atmosphere at 263 K, the dominant product is **4**. Notably, the single hydride signal seen for **4** appears at $\delta -2.4$ and couples to only three ^{31}P nuclei with $J_{PH} = 26$ Hz (triplet) and 36 Hz (doublet), respectively, as

shown in Figure 3a. This hydride resonance also possesses ^{183}W satellites with $J_{HW} = 28$ Hz. The three ^{31}P nuclei which couple to the hydride produced signals at $\delta 54.7$ (d) and 42.3 (td), while a third signal for an uncoordinated moiety is evident as a doublet with $J_{PP} = 38$ Hz at $\delta -12.4$; this resonance showed no coupling to the hydride ligands. The T_1 value of 0.89 s for the hydride ligands in **4**, at 228 K, is consistent with a high oxidation state and therefore classical hydride binding.²⁰ **4** must therefore be the 18 electron complex $W(H)_6(dppe-\kappa^2P)(dppe-\kappa^1P)$.

These conclusions are supported by the fact that the known nine coordinate hexahydride complex $W(H)_6(PMe_2Ph)_3$ has similar J_{PH} (36 Hz) and J_{WH} (27 Hz) to those observed for **4**.⁵¹ These data are therefore fully consistent with the proposed $W(VI)$ hexahydride formulation of **4** and we note the diagnostically low value of J_{WH} of 28 Hz compared with that of **2** (38 Hz).⁵¹

The photochemical procedure described above reached a photostationary state with **2** and **4** present in a 1:1 ratio and with no evidence for **3** found in the associated NMR spectra. Furthermore, there was no evidence of any net reaction when **2** was irradiated in the absence of H_2 . Repetition of the reaction of **2** with *para*- H_2 failed to produce PHIP in the hydride signals observed for either **2** or **4**. These results therefore suggest that UV irradiation of **2** under these conditions leads to phosphine dissociation rather than the H_2 loss suggested by others previously.⁵²

Additionally, when a sample of **4** is warmed with *para*- H_2 , no PHIP is evident in the detected hydride signals of **2**. This observation confirms that the displacement of H_2 and conversion of the $dppe-\kappa^1P$ ligand to its κ^2 form is intramolecular with respect to four of the six hydride ligands of **4**.

Formation of $W(H)_3(OH)(dppe-\kappa^2P)_2$ (5**).** In a number of these reactions, a further product was often observed but only if NMR solvents were used without drying.

When a wet toluene- d_8 solution of **1** was left overnight, slow decomposition occurs such that ^{31}P NMR signals for **2**, free $dppe$, the mono phosphine oxide of $dppe$ and a new complex **5** can be detected. In the 1H NMR spectrum, three new high-field signals for **5** dominate at $\delta -2.26$, $\delta -2.37$ and $\delta -3.00$. These signals, which occur in the hydride region, appear even though no H_2 has been explicitly added to the sample.

However, upon addition of *para*- H_2 to the same sample, the hydride signals at $\delta -2.26$, $\delta -2.37$, as well as a previously masked peak at $\delta 1.59$ (with a peak envelope of ca. 200 Hz which indicates the presence of several strong couplings to ^{31}P) all show PHIP polarization (Figure 3b). The signal at $\delta -3.00$ which possesses much smaller $^1H-^{31}P$ splittings is apparently unaffected by the addition of *para*- H_2 and when D_2O and *para*- H_2 were used as reagents, only the two signals at $\delta -2.26$, $\delta -2.37$ were polarized.

In an H_2O -containing sample, the same 1H NMR integral values were obtained for the three high field signals, the eight ethane bridge protons, and the resonance at $\delta 1.59$. Significantly, COSY spectroscopy revealed that the $\delta 1.59$ signal of **5** couples to the two hydride signals $\delta -2.26$ and $\delta -2.37$ while EXSY measurements confirm that the hydrogen atoms in these three sites undergo positional interchange. The resonance at $\delta -3.00$ is not involved in this process. In the corresponding $^1H-^{31}P$ HMQC measurement, values of $J_{PH} = 100, 30, \text{ and } 60$ Hz produce strong connections to the $\delta 1.59$ 1H NMR signal which is therefore confirmed as a W -hydride

resonance. The three high field resonances have T_1 values of 0.28, 0.28, and 0.74 s, respectively, at 268 K. Complex **5** yields a further 40 aromatic proton resonances that arise from eight distinct and intact phenyl rings. It also gives four ^{31}P NMR signals for tungsten-coordinated phosphorus centers that appear at δ 36.6, 45.5, 47.3 and 64.0.

The identity of **5** was secured through a combination of EXSY measurements that probed the behavior of the site yielding the δ -3.00 signal together with H_2O doping studies that were conducted in toluene- d_8 solution. For the doping studies, a sample of **1** was prepared and a 20-fold excess of dppe added prior to the addition of 5 μL of H_2O . Over a period of several days at room temperature, the conversion of **1** into **5** was observed. On the basis of ^{31}P signal integrations, 50% of **1** converted into **5** and a similar amount of $\text{PPh}_2\text{CH}_2\text{CH}_2\text{PPh}_2\text{P}(\text{O})$. At this stage no H_2 was evident in solution. Concurrent UV irradiation increased the rate of reaction while generating mainly **2** and **4** and free H_2 ; the addition of H_2O to a solution of **3** produced a mixture of **2** and **5**.

EXSY measurements revealed that magnetization transfer occurs from the protons giving rise to the δ -3.00 signal of **5** to those associated with the peak at δ 0.47, due to H_2O . This process was enhanced by increasing the water concentration. Collectively, these observations allow **5** to be identified as $\text{W}(\text{H})_3(\text{OH})(\text{dppe-}\kappa^2\text{P})_2$ where the rate data associated with the proton transfer step yield $\Delta H^\ddagger = 42 \pm 5 \text{ kJ mol}^{-1}$ and $\Delta S^\ddagger = -90.5 \pm 18 \text{ J K}^{-1} \text{ mol}^{-1}$. The protons giving rise to the δ 1.59 hydride signal also show exchange with H_2O in the EXSY data. In addition, the three hydride signals show evidence for positional exchange.

In support of the assignment of **5** as a tungsten hydroxide complex, it should be noted that the hydroxyl proton resonance of the related complex $\text{Cp}^*(\text{PMe}_3)\text{Ir}(\text{Ph})\text{OH}$ appears as a broad singlet at δ -3.1 while that of $\text{Ru}(\text{IMes})_2(\text{CO})_2(\text{OH})\text{H}$ appears at δ -3.75 .^{53,54} In contrast, the aquo complex $\text{W}(\text{CO})_3(\text{P}^i\text{Pr}_3)(\text{H}_2\text{O})$ yields a signal for the coordinated H_2O at δ 3.03.⁵⁵ Consequently, the δ -3.00 signal of **5** is consistent with that of a metal hydroxyl. This is further supported by the fact that the addition of D_2O results in the rapid loss of the $\text{W}(\text{OH})$ resonance of **5** with subsequent reaction with *para*- H_2 , yielding only the PHIP enhanced δ -2.26 and δ -2.37 signals.

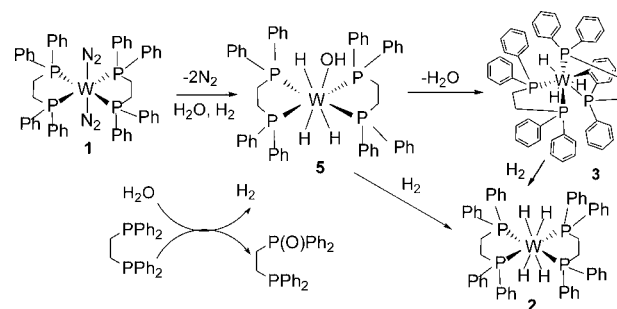
On a slower time scale, **5** converts thermally into **2** although ultimately in the presence of an excess of water only phosphine oxides of dppe remain according to ^{31}P NMR spectroscopy. This is consistent with the slow reductive elimination of H_2O from the metal center in **5** and subsequent reaction to form **2** or **3** as shown in Scheme 4. These observations also reveal that the 16 electron fragment $\text{W}(\text{H})_2(\text{dppe-}\kappa^2\text{P})_2$ is capable of intramolecular CH bond activation, in agreement with the DFT study discussed earlier.

Diffusion Ordered Spectroscopy. To confirm that these signals all originate from molecules with similar masses, a series of DOSY measurements were undertaken. These resulted in similar diffusion coefficients for **2**, **3**, **4**, and **5**, thereby confirming our mononuclear hypothesis, as illustrated in Table 4.

CONCLUSIONS

The conversion of $\text{W}(\text{N}_2)_2(\text{dppe-}\kappa^2\text{P})_2$ (**1**) into $\text{W}(\text{H})_4(\text{dppe-}\kappa^2\text{P})_2$ (**2**) has been shown to involve the initial formation of the *ortho*-metalated CH activation product $[\text{WH}_3\{\text{Ph}(\text{C}_6\text{H}_4)\text{-PCH}_2\text{CH}_2\text{PPh}_2\text{-}\kappa^2\text{P}\}(\text{dppe-}\kappa^2\text{P})]$ (**3**). Caulton et al. prepared

Scheme 4. Conversion of **1** to **2** Where H_2O Can Act as the Source of H_2 ^a



^aThese transformations can be initiated thermally and photochemically.

Table 4. Diffusion Data for **2**, **3**, **4**, and **5**

complex, solvent, and temperature	resonance / δ	diffusion coefficient (cm^2/s)
2 , THF, 293 K	-3.94	1.27
3 , THF, 293 K	-0.25	1.50
	-2.98	1.50
	-3.12	1.50
4 , THF, 293 K	-2.85	2.42
5 , Toluene, 273 K	-2.29	0.57
	-2.40	0.57
	-3.00	0.57

the related complex $\text{W}(\text{H})_3(\eta^2\text{-C}_6\text{H}_4\text{PMe}_2)(\text{PMe}_2\text{Ph})_3$ from $\text{WH}_2\text{Cl}_2(\text{PMe}_2\text{Ph})_4$ via reaction with $^t\text{BuLi}$.⁵⁶ Furthermore, Hidai et al. have speculated that warming benzene solutions of **1** to reflux leads to the formation of *meso*- o - $\text{C}_6\text{H}_4(\text{PPhCH}_2\text{CH}_2\text{PPh}_2)_2$ via the proposed reaction intermediate $[\text{WH}\{\text{Ph}(\text{C}_6\text{H}_4)\text{PCH}_2\text{CH}_2\text{PPh}_2\text{-}\kappa^2\text{P}\}(\text{dppe-}\kappa^2\text{P})]$; we note that some of their reported NMR data¹⁰ appear to match that presented here for **3**. The observation of a CH bond activation pathway during the formation of **2** is therefore entirely consistent with the known chemistry of related systems.

The theoretical studies used $\text{W}(\text{N}_2)_2((\text{Ph})\text{HPCH}_2\text{CH}_2\text{PH}_2\text{-}\kappa^2\text{P})(\text{H}_2\text{PCH}_2\text{CH}_2\text{PH}_2\text{-}\kappa^2\text{P})$ (**1m**) as a starting point from which to explore these reactions. They revealed that N_2 loss leads to $\text{W}(\text{N}_2)((\text{Ph})\text{HPCH}_2\text{CH}_2\text{PH}_2\text{-}\kappa^2\text{P})(\text{H}_2\text{PCH}_2\text{CH}_2\text{PH}_2\text{-}\kappa^2\text{P})$ (**6m**³) which exists as a triplet unless explicitly solvated by two molecules of THF. *ortho*-Metalation and H_2 addition were both shown to be feasible reaction steps prior to the formation of **3** and **2**, respectively. These results therefore rationalized the observation of both **3** and **2** in the reaction chemistry of **1**. They also help explain the detection of PHIP in the corresponding reaction products.

The trapping of hydrogen by organometallic complexes and the reverse process have proven important in energy storage applications.⁵⁷ It has been demonstrated in this work that $\text{W}(\text{N}_2)_2(\text{dppe-}\kappa^2\text{P})_2$ (**2**) is capable of releasing H_2 from H_2O in conjunction with the formation of a phosphine oxide and ultimately $\text{W}(\text{H})_4(\text{dppe-}\kappa^2\text{P})_2$ (**2**). This transformation involves the metal hydroxyl-hydride complex $\text{W}(\text{H})_3(\text{OH})(\text{dppe-}\kappa^2\text{P})_2$ (**5**) via the reaction sequence illustrated in Scheme 4. Such species have been shown to play a role in organic oxidations.⁵⁸ This reaction therefore illustrates a route to H_2 production from H_2O facilitated, in this case by phosphorus acting as a suitable oxygen acceptor.

When these reactions are conducted with *para*-H₂, PHIP is evident in the hydride signals of **2**, **3** and **5**. This confirms the utility of PHIP as a powerful method for examining the reactivity of polyhydride complexes of this type. Furthermore, the experimental and computation results also suggest that nonclassical dihydride complexes do not play a significant role in the oxidative addition process. In contrast, H₂ addition to W(CO)₃(PCy₃)₂ was shown not to produce detectable PHIP in the W(H)₂(CO)₃(PCy₃)₂ product. In this latter case, a role for a nonclassical dihydrogen complex in the addition process has been well established.^{5–5} The postulation here that **3** and **4** exist as classical W(IV) and W(VI) species was further supported by the long T_{1(min)} values of the hydride ligands (>0.3 s), the observation of appropriate J_{HW} couplings and the detection of ¹⁸³W signals for **2**, **3** and **4**. The ¹⁸³W resonance for W(VI) **4** appears at the high field value of δ —4000, in accordance with its high oxidation state. This compares with values of δ —3363 for **2** and δ —2913 for **3** both of which complexes exist as W(IV) species. Attempts to locate the corresponding signal in **5** failed, presumably as a consequence of its dynamic behavior leading to signal broadening.

It has previously been reported that UV irradiation of W(H)₄(dppe-κ²P)₂ under N₂ leads to low yields of ammonia⁵⁹ and alkene hydrogenation. It has also been reported that H₂ loss corresponds to the main photochemical process in such systems.^{50,52} Here we have demonstrated that W(H)₆(dppe-κ²P)(dppe-κ¹P) (**4**) is formed under UV irradiation which suggests that 16-electron W(H)₄(dppe-κ²P)(dppe-κ¹P) and not W(H)₂(dppe-κ²P)₂ is responsible for these conversions.

Thus, the results presented here demonstrate that CH bond activation, phosphine dechelation, and the oxidative addition of OH bonds are all important in the chemistry of W(N₂)₂(dppe-κ²P)₂ (**1**).

■ ASSOCIATED CONTENT

Supporting Information

Characterization of **3** and **5**, and the DFT derived energetics and coordinates for all the species discussed. This material is available free of charge via the Internet at <http://pubs.acs.org>.

■ AUTHOR INFORMATION

Corresponding Author

sbd3@york.ac.uk

Notes

The authors declare no competing financial interest.

■ ACKNOWLEDGMENTS

We are grateful for financial support from the BBSRC (P.J.C.), AstraZeneca and the Spanish MEC Consolider Ingenio 2010-ORFEO-CSD2007-00006 (B.E.) research programme. We also thank Professor Robin Perutz for helpful discussions.

■ REFERENCES

- (1) Bell, B.; Chatt, J.; Leigh, G. J. *J. Chem. Soc., Dalton Trans.* **1972**, 2492.
- (2) Hidai, M.; Mizobe, Y. *Chem. Rev.* **1995**, *95*, 1115.
- (3) Kubas, G. J.; Unkefer, C. J.; Swanson, B. I.; Fukushima, E. *J. Am. Chem. Soc.* **1986**, *108*, 7000.
- (4) Khalsa, G. R. K.; Kubas, G. J.; Unkefer, C. J.; Vandersluys, L. S.; Kubatmartin, K. A. *J. Am. Chem. Soc.* **1990**, *112*, 3855.
- (5) Kubas, G. J.; Ryan, R. R.; Swanson, B. I.; Vergamini, P. J.; Wasserman, H. J. *J. Am. Chem. Soc.* **1984**, *106*, 451.
- (6) Heinekey, D. M.; Oldham, W. J. *Chem. Rev.* **1993**, *93*, 913.

- (7) Bell, B.; Chatt, J.; Leigh, G. J. *J. Chem. Soc. D* **1970**, 842.
- (8) Ishida, T.; Mizobe, Y.; Tanase, T.; Hidai, M. *J. Organomet. Chem.* **1991**, *409*, 355.
- (9) Seino, H.; Arita, C.; Nonokawa, D.; Nakamura, G.; Harada, Y.; Mizobe, Y.; Hidai, M. *Organometallics* **1999**, *18*, 4165.
- (10) Arita, C.; Seino, H.; Mizobe, Y.; Hidai, M. *Bull. Chem. Soc. Jpn.* **2001**, *74*, S61.
- (11) Sattler, A.; Parkin, G. *Nature* **2010**, *463*, 523.
- (12) Chatt, J.; Pearman, A. J.; Richards, R. L. *J. Chem. Soc., Dalton Trans.* **1977**, 2139.
- (13) Jia, G.; Morris, R. H.; Schweitzer, C. T. *Inorg. Chem.* **1991**, *30*, 593.
- (14) Nishibayashi, Y.; Iwai, S.; Hidai, M. *Science* **1998**, *279*, 540.
- (15) Nishibayashi, Y.; Takemoto, S.; Iwai, S.; Hidai, M. *Inorg. Chem.* **2000**, *39*, 5946.
- (16) Hlatky, G. G.; Crabtree, R. H. *Coord. Chem. Rev.* **1985**, *65*, 1.
- (17) Crabtree, R. H.; Lavin, M. *J. Chem. Soc., Chem. Commun.* **1985**, 1661.
- (18) Hamilton, D. G.; Crabtree, R. H. *J. Am. Chem. Soc.* **1988**, *110*, 4126.
- (19) Ammann, C.; Isaia, F.; Pregosin, P. S. *Magn. Reson. Chem.* **1988**, *26*, 236.
- (20) Michos, D.; Luo, X. L.; Faller, J. W.; Crabtree, R. H. *Inorg. Chem.* **1993**, *32*, 1370.
- (21) Oglieve, K. E.; Henderson, R. A. *J. Chem. Soc., Chem. Commun.* **1992**, 441.
- (22) Muckerman, J. T.; Fujita, E.; Hoff, C. D.; Kubas, G. J. *J. Phys. Chem. B* **2007**, *111*, 6815.
- (23) Li, J.; Yoshizawa, K. *Chem.—Eur. J.* **2012**, *18*, 783.
- (24) Maseras, F.; Lledos, A.; Clot, E.; Eisenstein, O. *Chem. Rev.* **2000**, *100*, 601.
- (25) Balu, P.; Baskaran, S.; Kannappan, V.; Sivasankar, C. *Polyhedron* **2012**, *31*, 676.
- (26) Sandhya, K. S.; Suresh, C. H. *Dalton Trans.* **2012**, *41*, 11018.
- (27) Ball, G. E.; Brookes, C. M.; Cowan, A. J.; Darwish, T. A.; George, M. W.; Kawanami, H. K.; Portius, P.; Rourke, J. P. *Proc. Natl. Acad. Sci. U.S.A.* **2007**, *104*, 6927.
- (28) Geftakis, S.; Ball, G. E. *J. Am. Chem. Soc.* **1999**, *121*, 6336.
- (29) Ball, G. E.; Darwish, T. A.; Geftakis, S.; George, M. W.; Lawes, D. J.; Portius, P.; Rourke, J. P. *Proc. Natl. Acad. Sci. U.S.A.* **2005**, *102*, 1853.
- (30) Cunningham, J. L.; Duckett, S. B. *Dalton Trans.* **2005**, 744.
- (31) Matthews, S. L.; Heinekey, D. M. *J. Am. Chem. Soc.* **2006**, *128*, 2615.
- (32) Lyon, C. E.; Suh, E. S.; Dobson, C. M.; Hore, P. J. *J. Am. Chem. Soc.* **2002**, *124*, 13018.
- (33) Blazina, D.; Dunne, J. P.; Aiken, S.; Duckett, S. B.; Elkington, C.; McGrady, J. E.; Poli, R.; Walton, S. J.; Anwar, M. S.; Jones, J. A.; Carteret, H. A. *Dalton Trans.* **2006**, 2072.
- (34) Dunne, J. P.; Blazina, D.; Aiken, S.; Carteret, H. A.; Duckett, S. B.; Jones, J. A.; Poli, R.; Whitwood, A. C. *Dalton Trans.* **2004**, 3616.
- (35) Anwar, M. S.; Blazina, D.; Carteret, H. A.; Duckett, S. B.; Halstead, T. K.; Jones, J. A.; Kozak, C. M.; Taylor, R. J. K. *Phys. Rev. Lett.* **2004**, *93*, No. 040501.
- (36) Duckett, S. B.; Mewis, R. E. *Acc. Chem. Res.* **2012**, *45*, 1247.
- (37) Benn, R.; Brenneke, H.; Heck, J.; Rufinska, A. *Inorg. Chem.* **1987**, *26*, 2826.
- (38) Carlton, L.; Emdin, A.; Lemmerer, A.; Fernandes, M. A. *Magn. Reson. Chem.* **2008**, *46*, S56.
- (39) Crabtree, R. H.; Hlatky, G. G. *Inorg. Chem.* **1982**, *21*, 1273.
- (40) Thomas, A.; Haake, M.; Grevels, F. W.; Bargon, J. *Angew. Chem., Int. Ed. Engl.* **1994**, *33*, 755.
- (41) Thomas, R. J. W.; Laurence, G. S.; Diamantis, A. A. *Inorg. Chim. Acta* **1978**, *30*, L353.
- (42) Carlton, L.; Emdin, A.; Lemmerer, A.; Fernandes, M. A. *Magn. Reson. Chem.* **2008**, *46*, S56.
- (43) Schott, D.; Sleigh, C. J.; Lowe, J. P.; Duckett, S. B.; Mawby, R. J.; Partridge, M. G. *Inorg. Chem.* **2002**, *41*, 2960.
- (44) Duckett, S. B.; Wood, N. J. *Coord. Chem. Rev.* **2008**, *252*, 2278.

- (45) Desrosiers, P. J.; Cai, L. H.; Lin, Z. R.; Richards, R.; Halpern, J. J. *Am. Chem. Soc.* **1991**, *113*, 4173.
- (46) Archer, L. J.; George, T. A. *Inorg. Chim. Acta, Lett.* **1980**, *44*, L129.
- (47) Mohr, F.; Priver, S. H.; Bhargava, S. K.; Bennett, M. A. *Coord. Chem. Rev.* **2006**, *250*, 1851.
- (48) Macgregor, S. A.; Eisenstein, O.; Whittlesey, M. K.; Perutz, R. N. *J. Chem. Soc., Dalton Trans.* **1998**, 291.
- (49) Schott, D.; Callaghan, P.; Dunne, J.; Duckett, S. B.; Godard, C.; Goicoechea, J. M.; Harvey, J. N.; Lowe, J. P.; Mawby, R. J.; Muller, G.; Perutz, R. N.; Poli, R.; Whittlesey, M. K. *Dalton Trans.* **2004**, 3218.
- (50) Pivovarov, A. P. *Russ. Chem. Bull.* **2008**, *57*, 289.
- (51) Crabtree, R. H.; Hlatky, G. G. *Inorg. Chem.* **1984**, *23*, 2388.
- (52) Graff, J. L.; Sobieralski, T. J.; Wrighton, M. S.; Geoffroy, G. L. *J. Am. Chem. Soc.* **1982**, *104*, 7526.
- (53) Woerpel, K. A.; Bergman, R. G. *J. Am. Chem. Soc.* **1993**, *115*, 7888.
- (54) Jazzar, R. F. R.; Bhatia, P. H.; Mahon, M. F.; Whittlesey, M. K. *Organometallics* **2003**, *22*, 670.
- (55) Kubas, G. J.; Burns, C. J.; Khalsa, G. R. K.; Vandersluys, L. S.; Kiss, G.; Hoff, C. D. *Organometallics* **1992**, *11*, 3390.
- (56) Rothfuss, H.; Huffman, J. C.; Caulton, K. G. *Inorg. Chem.* **1994**, *33*, 2946.
- (57) Kubas, G. J. *J. Organomet. Chem.* **2009**, *694*, 2648.
- (58) Bryndza, H. E.; Tam, W. *Chem. Rev.* **1988**, *88*, 1163.
- (59) Dziegielewska, J. O.; Gilbertowska, R.; Mrzigod, J.; Malecki, J. *G. Polyhedron* **1995**, *14*, 1375.